Magnetic-Photoluminescent Nanoplatform Built from Large-Pore Mesoporous Silica

Fan Yang[†], Artiom Skripka[†], Maryam Sadat Tabatabaei[‡], Sung Hwa Hong[¶], Fuqiang Ren[†], Yue Huang[†], Jung Kwon Oh[¶], Sylvain Martel[‡], Xinyu Liu[§], Fiorenzo Vetrone[*,†], Dongling Ma[*,†]

[†] Institut National de la Recherche Scientifique, Centre Énergie, Matériaux et Télécommunications, Université du Québec, 1650 Boul. Lionel-Boulet, Varennes, Québec J3X 1S2, Canada

[‡] NanoRobotics Laboratory, Department of Computer and Software Engineering, Institute of Biomedical Engineering, Polytechnique Montréal, Montréal, QC H3T 1J4, Canada

[¶] Department of Chemistry and Biochemistry, Concordia University, Montreal, Quebec H4B 1R6, Canada

[§] Department of Mechanical and Industrial Engineering, University of Toronto, 5 King's College Road, Toronto, Ontario, M5S 3G8, Canada

Supporting information

Experimental section

Chemicals

Iron chloride hexahydrate ($FeCl_3.6H_2O$), sodium oleate, oleic acid (OA, technical grade 90%), 1-Tetradecene (TDE, technical grade 92%), 1-Octadecene (ODE, technical grade 90%), ammonium hydroxide solution ($NH_3.H_2O$, 28.0~30.0% ammonia content), tetraethyl orthosilicate (TEOS, 99.999%), (3-mercaptopropyl)trimethoxysilane (MPTS, 95%), triethanolamine (TEA), cetyltrimethylammonium chloride solution (CTAC, 25 wt% in H_2O), lead chloride ($PbCl_2$, 98%), sulfur (S, 100%), oleylamine (OLA, technical grade, 70%), cadmium oxide (CdO, 99%), ammonium nitrate (NH_4NO_3), branched polyethylenimine (PEI, Mw $\approx$ 25 000), doxorubicin hydrochloride (DOX) and phosphate buffered saline (PBS) were purchased from Sigma-Aldrich Inc. Hexane, toluene, chloroform, cyclohexane and ethanol were purchased from Fisher Scientific Company. All chemicals were used as purchased.

Synthesis of ultrasmall Fe_3O_4 magnetic nanoparticles (NPs)

Fe_3O_4 NPs were synthesized by a modified thermal decomposition method according to a previous report.[1] Typically, iron oleate precursor was prepared by refluxing $FeCl_3.6H_2O$ (1.08 g, 4 mmol) and sodium oleate (4.87 g, 16 mmol) in a mixture solution of ethanol (8 mL), distilled water (6 mL) and hexane (14 mL) at 70 ℃ for 6 h. The iron oleate precursor was then separated by a funnel and washed several times. After that, the iron oleate precursor (0.9 g, 1 mmol) was dissolved in a mixture of OA (142 mg, 0.5 mmol), TDE (1.75 g, 9 mmol) and ODE (3.25 g, 13 mmol), then heated to 290 ℃ under N_2 flow for 1 h. Finally, the Fe_3O_4 NPs were precipitated by adding ethanol and dispersed in chloroform as stock solution.

Synthesis of PbS quantum dots (QDs)

PbS QDs were synthesized by a hot-injection method.[2, 3] In a typical reaction, $PbCl_2$ (10 g) and OLA (24 mL) were added into a 50 mL flask and heated to 160 ℃ for 1 h. The $PbCl_2$-OLA solution was then cooled to 120 ℃ under vacuum for 30 min. Subsequently, sulfur (115 mg) in OLA (4

mL) was quickly injected into the above $PbCl_2$-OLA solution under N_2 flow. The growth reaction of PbS QDs was kept at 100 ℃ for several min to reach the desired size. The reaction was quenched by cold water, followed by adding ethanol and toluene to purify the PbS QDs. Finally, the PbS QDs were dispersed in toluene for the further growth of CdS shell.

Synthesis of PbS/CdS core/shell QDs

PbS/CdS QDs were synthesized by a microwave-assisted cation exchange method.[3] Briefly, CdO (3 g), OA (15 mL) and ODE (20 mL) were heated to 200 ℃ to prepare the Cd precursor solution. The solution was then cooled to 100 ℃ and degassed under vacuum for 30 min. The temperature was further decreased to 30 ℃ and 12 mL of PbS QDs in toluene was added via a syringe. Then 20 mL of the mixed solution was introduced into a 35 mL microwave reaction tube and heated at 100 ℃ under microwave radiation for several min. Finally, PbS/CdS QDs were purified by repeated precipitation and re-dispersion.

Synthesis of large-pore mesoporous silica nanospheres ($mSiO_2$)

The 3-demensional dendritic $mSiO_2$ particles were prepared by a one-pot biphase stratification method.[4] Typically, CTAC solution (12 mL 25 wt%) and TEA (0.09 g) were added into distilled water (18 mL) and stirred at 60 ℃ in an oil bath for 1 h. Then TEOS (0.5 mL) in cyclohexane (9.5 mL) was gently added to the above mixed solution. The reaction was kept at 60 ℃ for 60 h. The resulting products were collected by centrifugation and washed several times with ethanol. At last, the products were extracted with 0.6 wt% NH_4NO_3 ethanol solution at 60 ℃ for 6 h twice to remove the CTAC template completely, and dispersed in ethanol.

Synthesis of thiol-modified mesoporous silica nanospheres ($mSiO_2$-SH)

For surface modification with thiol groups, $mSiO_2$ (300 mg) in 15 mL of ethanol was added with 150 μL of MPTS and 375 μL of $NH_3.H_2O$, followed by vigorous stirring for 12 h at room temperature. The final products of $mSiO_2$-SH were washed with ethanol several times and dispersed in chloroform.

Synthesis of Fe_3O_4 and PbS/CdS loaded $mSiO_2$ ($mSiO_2$@PbS/CdS-Fe_3O_4)

Briefly, 1mL of Fe_3O_4 and PbS/CdS (4 mg/mL)-in-chloroform solution was added into 4 mL of $mSiO_2$-SH chloroform solution (2 mg/mL) and stirred at room temperature for 30 min. The loading ratio can be simply controlled by varying the volume of Fe_3O_4 and PbS/CdS chloroform solution. The $mSiO_2$@PbS/CdS-Fe_3O_4 particles were then retrieved by centrifugation and washed by chloroform once to remove free, not-loaded Fe_3O_4 NPs and PbS/CdS QDs. Subsequently, 1 mL of $mSiO_2$@PbS/CdS-Fe_3O_4 in chloroform dispersion (5 mg/mL) was mixed with 20 mg of PEI and stirred for 2 h to transfer the $mSiO_2$@PbS/CdS-Fe_3O_4 into water by forming a PEI coating. Finally, the PEI-coated $mSiO_2$@PbS/CdS-Fe_3O_4 particles were precipitated by adding cyclohexane and re-dispersed in water.

Structural, magnetic and optical characterizations

X-Ray Diffraction (XRD) pattern was acquired using a Bruker D8 ADVANCE X-ray diffractometer equipped with Cu anode X-ray source (Cu-kα, λ=1.540598 Å). The morphology of

as-prepared NPs was investigated by transmission electron microscopy (TEM, JEOL 2100F) at 200 kV equipped with a charge-coupled device (CCD) camera. Energy Dispersive X-ray Spectroscopy (EDX) was taken on specific areas during TEM measurements. Absorption spectra were taken by a UV-visible-NIR spectrophotometer (Cary 5000) with a scan speed of 600 nm/min. Photoluminescence (PL) spectra were acquired on a Fluorolog®-3 system (Horiba Jobin Yvon) using an excitation wavelength of 600 nm. Fourier-transform infrared (FTIR) spectra were recorded by a ThermoFisher Scientific Nicolet 6700 FTIR spectrometer using KBr as a reference. The nitrogen adsorption-desorption isotherms were measured using Quantachrome Autosorb-1 Automated Gas Sorption System Analyzer. Specific surface areas and pore size distributions were calculated based on BET (Brunauer-Emmett-Teller) measurements and density functional theory (DFT) method. The loading content of Fe_3O_4 NPs and PbS/CdS QDs was determined by inductively coupled plasma-optical emission spectrometry (ICP-OES) (Agilent Technologies, 5100). Magnetic hysteresis loop was measured by a vibrating sample magnetometer (VSM, Model 4 HF-VSM, ADE USA) at 300 K with magnetic field up to 3 T. Temperature-dependence ZFC and FC magnetization curves were taken under an applied field of 100 Oe between 5 K and 300 K.

Cell culture and viability assay of $mSiO_2$@PbS/CdS-Fe_3O_4

HeLa cancer cells and human embryonic kidney (HEK 293T) cells were cultured in Dulbecco's modified Eagle's medium (DMEM) containing 10% fetal bovine serum (FBS), 50 units/mL penicillin and 50 units/mL streptomycin in 5% CO_2 at 37 °C. HEK 293T and HeLa cells were plated into a 96-well plate with a density of 5×10^5 cells/well and incubated for 24 h in DMEM (100 μL). Various concentrations of $mSiO_2$@PbS/CdS-Fe_3O_4 were then added into the plate. Blank controls without $mSiO_2$@PbS/CdS-Fe_3O_4 (*i.e.*, cells only) were run simultaneously. Cell viability was measured using CellTiter 96 Non-Radioactive Cell Proliferation Assay kit (MTT, Promega) according to the manufacturer's protocol. Briefly, 3-(4,5-dimethylthiazol-2-yl)-2,5-diphenyltetrazolium bromide (MTT) solution (15 μL) was added into each well. After 24 h incubation, the medium containing unreacted MTT was carefully removed. Dimethyl sulfoxide (DMSO, 100 μL) was added into each well in order to dissolve the formed formazan blue crystals, and then the absorbance at $\lambda = 570$ nm was recorded using a Powerwave HT Microplate Reader (Bio-Tek). Each concentration was 6-replicated (n = 6). Cell viability was calculated as the ratio of absorbance of mixtures containing $mSiO_2$@PbS/CdS-Fe_3O_4 to control cells.

DOX loading and pH/MF/NIR-responsive drug release

DOX loading: 5 mL of $mSiO_2$@PbS/CdS-Fe_3O_4 samples (2 mg/mL) were mixed with 2 mL of DOX solution in PBS buffer (1mg/mL) under magnetic stirring for 24 h. Then the $mSiO_2$@PbS/CdS-Fe_3O_4/DOX particles were separated by centrifugation and washed with PBS buffer. To evaluate the DOX loading efficiency, the supernatant and washed solutions were collected and the residual DOX content was measured by a UV-Vis absorption spectrophotometer at wavelength of 480 nm. The loading efficiency (LE) can be calculated as following:

$$\mathrm{LE} = \frac{O_{DOX} - R_{DOX}}{O_{DOX}}$$

Where O_{DOX} is original DOX content, R_{DOX} is residual DOX content in collected supernatant and washed solution by centrifugation.

pH-responsive DOX release: $mSiO_2$@PbS/CdS-Fe_3O_4/DOX particles were immersed in 2 mL of PBS in a flask (pH= 7.4/5.0) with gentle stirring. At certain time intervals, the supernatant was taken out by centrifugation to measure the concentration of released DOX and fresh PBS was added again for further drug release experiments.

Magnetic field-responsive DOX release: The same procedure as pH-responsive DOX release was adopted except for putting the flask containing $mSiO_2$@PbS/CdS-Fe_3O_4/DOX under magnetic field (MF). The MF was generated by magnetothermal equipment (Ameritherm Inc., New York) consisting of 3 turns of copper coil (6 cm in diameter) with a water-cooling circuit. The MF frequency of the equipment is 150 kHz as default setting and MF amplitude could be tuned by the current in the range of 0~180 A. MF (*H*) was calculated by the following equation:

$$H = n\frac{\mu_0 I}{2R},$$

where μ_0 = 4π×10^{-7} T.m/A, n is the number of turns, *R* is the loop radius and *I* is the applied current. In our experiment, the current was set as 100 A and *H* was estimated to be 5 kA/m.

NIR-responsive DOX release: The stimulus of pH was replaced by an 806 nm continuous NIR laser (power density of 1.3 W/cm^2) while other setups were kept the same.

The temperature increase during the drug release was recorded by a computer attached optical fibre based thermocouple (Reflex, SN:T18 217A, Neoptix Inc, Canada).

Thermal images were recorded by an infrared thermal imaging camera (FLIR E4, FLIR systems AB, Sweden).

NIR imaging *ex vivo* and photoluminescence signal penetration depth

We designed an experimental setup to acquire NIR images *ex vivo* and estimate the photoluminescence penetration depth, in which the $mSiO_2$@PbS/CdS-Fe_3O_4 aqueous solution was filled in a cuvette underneath a piece of pork tissue of different thickness. NIR images were recorded by a Xeva-1.7 infrared camera (Xenics Corp, Belgium) equipped with a 830 nm long-pass optical filter to block the light below 830 nm and the scattered excitation light of the 806 nm laser. The laser diode of 806 nm with power density of 10 W/cm^2 was used as excitation source.

Animal model

4T1 murine breast cancer cells were cultured in standard cell media recommended by American type culture collection (ATCC). Female Balb/C mice were purchased from Nanjing Peng Sheng Biological Technology Co Ltd and used under approved protocols approved by Soochow University Laboratory Animal Center.

T_2 relaxivity study *in vitro* and MR imaging *in vivo*

T_2-weighted MR images were acquired by a 3T clinical MRI scanner (Bruker Biospin Corporation, Billerica, MA, USA) at room temperature. The $mSiO_2$@PbS/CdS-Fe_3O_4 particles dispersed in PBS buffer at different concentrations were placed in tubes for T_2-weighted MR imaging. The concentration of Fe was determined by inductively coupled plasma-optical emission spectrometry (ICP-OES). Relaxivity (r_2) values were calculated by fitting the curve of $1/T_2$ relaxation time (s^{-1}) vs the concentration of Fe (mM).

For *in vivo* MR imaging, $mSiO_2$@PbS/CdS-Fe_3O_4 dispersed in PBS buffer (200 μL, 2 mg/mL) were injected into mice bearing 4T1 tumors. MR imaging of the mouse was conducted on the same scanner equipped with a special coil designed for small animal imaging. The mouse was scanned before and after injection of the contrast agent.

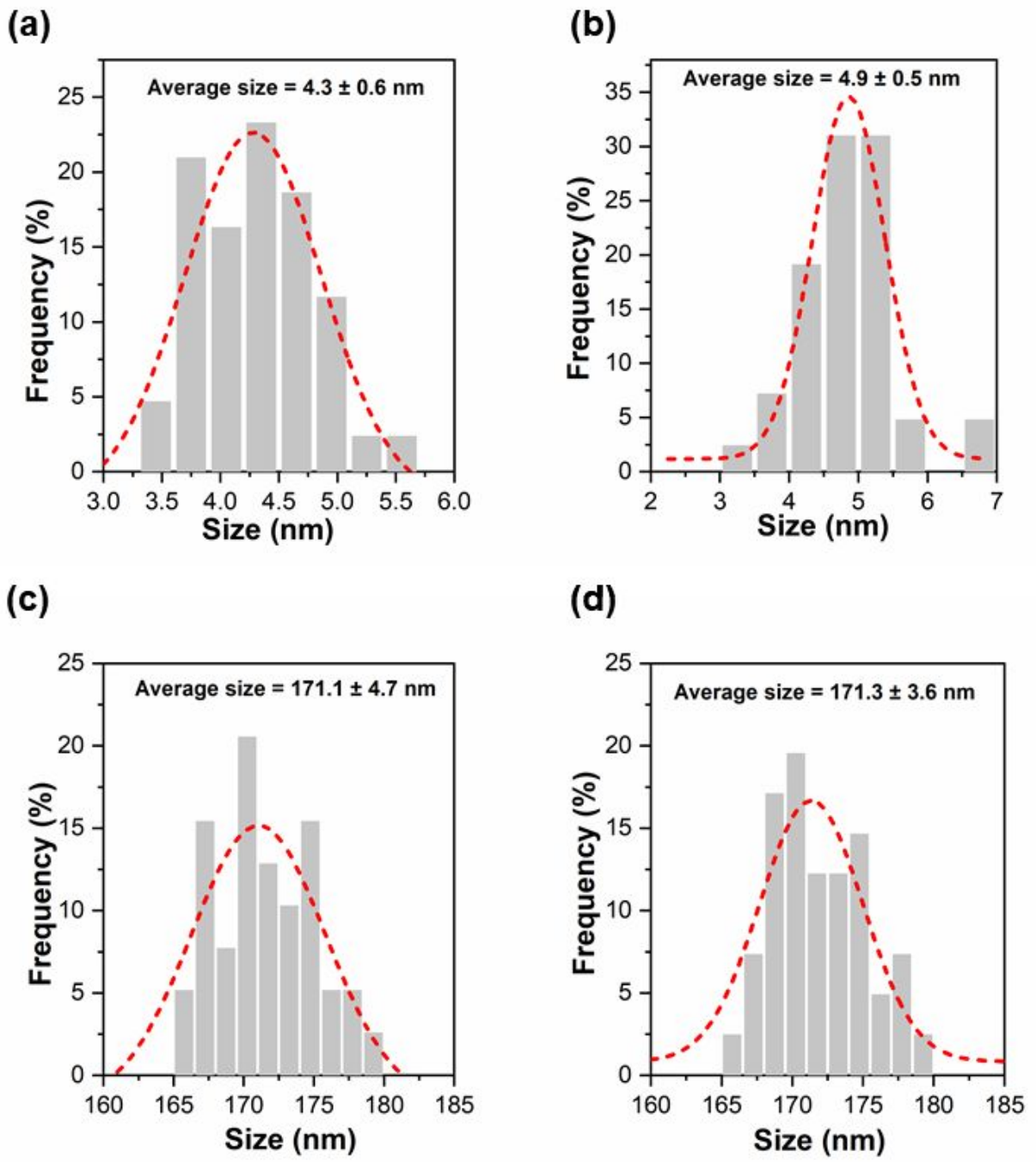

Figure S1 Size distribution histogram of (a) PbS/CdS QDs, (b) Fe_3O_4 NPs, (c) $mSiO_2$ and (d) $mSiO_2$@PbS/CdS-Fe_3O_4.

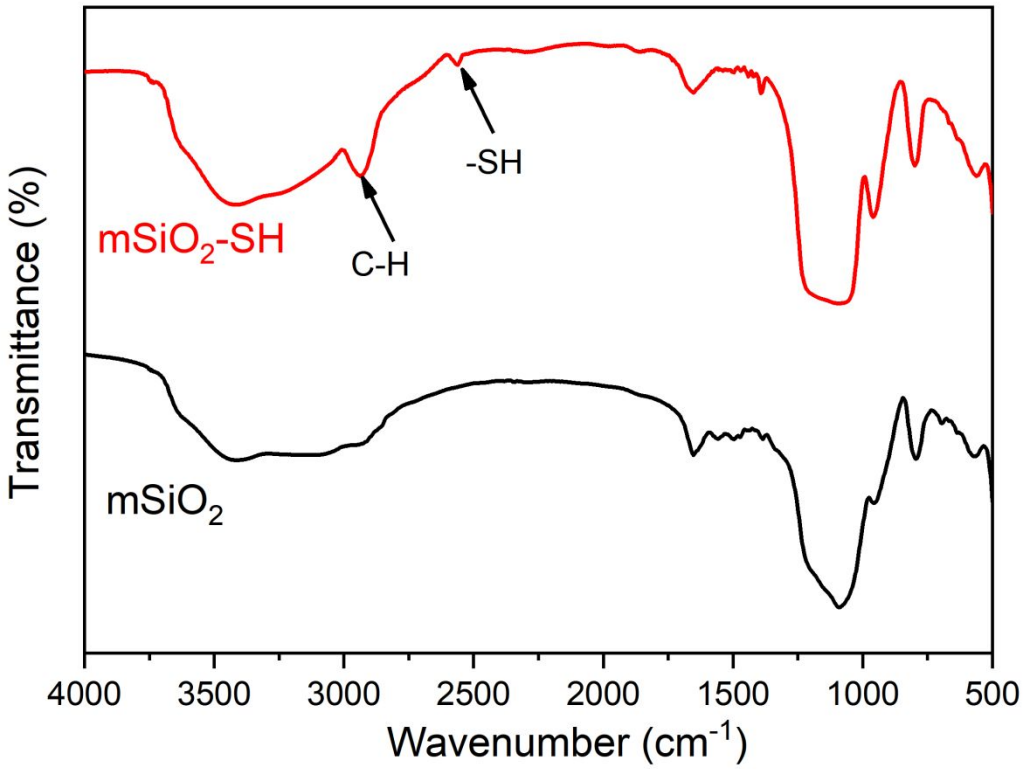

Figure S2 FTIR spectra of $mSiO_2$ and thiol-modified $mSiO_2$ (denoted as $mSiO_2$-SH herein). The peaks at 2940 and 2560 cm^{-1} are assigned to the C-H and -SH stretching modes,[5] which indicates the grafting of thiol groups onto $mSiO_2$ after MPTS modification.

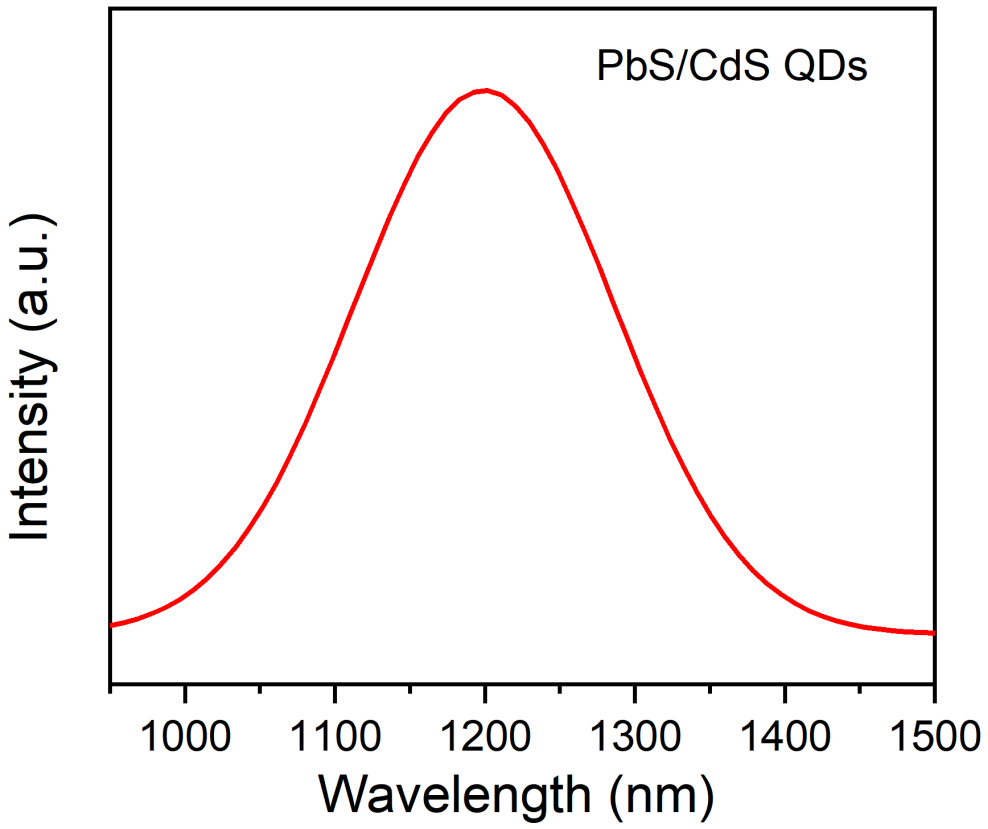

Figure S3 NIR photoluminescence spectrum of PbS/CdS QDs.

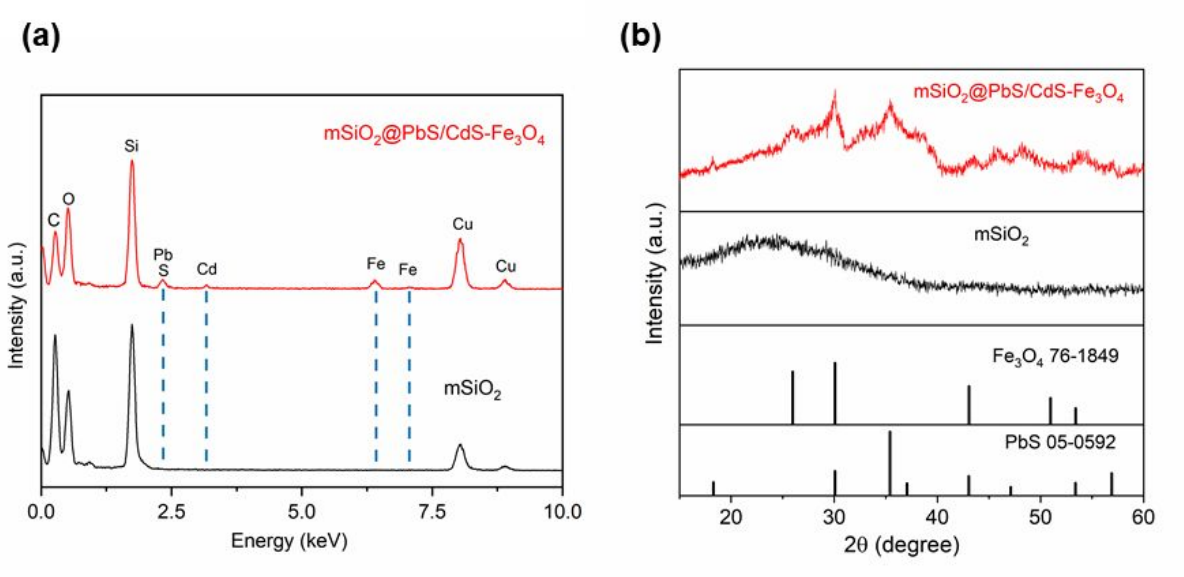

Figure S4 EDX spectra (a) and XRD patterns (b) of $mSiO_2$ and $mSiO_2$@PbS/CdS-Fe_3O_4. The EDX spectrum of $mSiO_2$@PbS/CdS-Fe_3O_4 shows the co-existence of Si, O, Fe, Pb, Cd and S elements whereas that of $mSiO_2$ only shows the composition of Si and O elements. It should be noted that Cu/C elements are from carbon film-covered-copper TEM grids. In addition, the XRD pattern of $mSiO_2$@PbS/CdS-Fe_3O_4 exhibits the characteristic diffraction peaks of PbS and Fe_3O_4 while that of $mSiO_2$ only exhibits the broad peak of amorphous silica. These results indicate that $mSiO_2$@PbS/CdS-Fe_3O_4 consist of Fe_3O_4 NPs and PbS/CdS QDs.

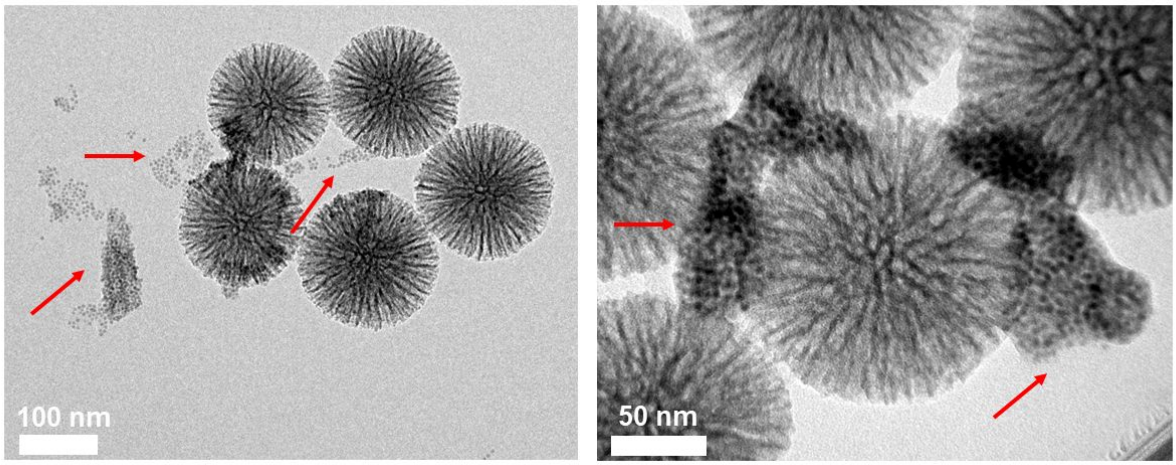

Figure S5 TEM images of the sample after the loading experiment of Fe_3O_4 NPs and PbS/CdS QDs into pure (not thiol-modified) $mSiO_2$. The red arrows indicate the unloaded Fe_3O_4 NPs and PbS/CdS QDs. It can be seen that the Fe_3O_4 NPs and PbS/CdS QDs cannot be efficiently immobilized into mesoporous channels of pure $mSiO_2$ without thiol modification.

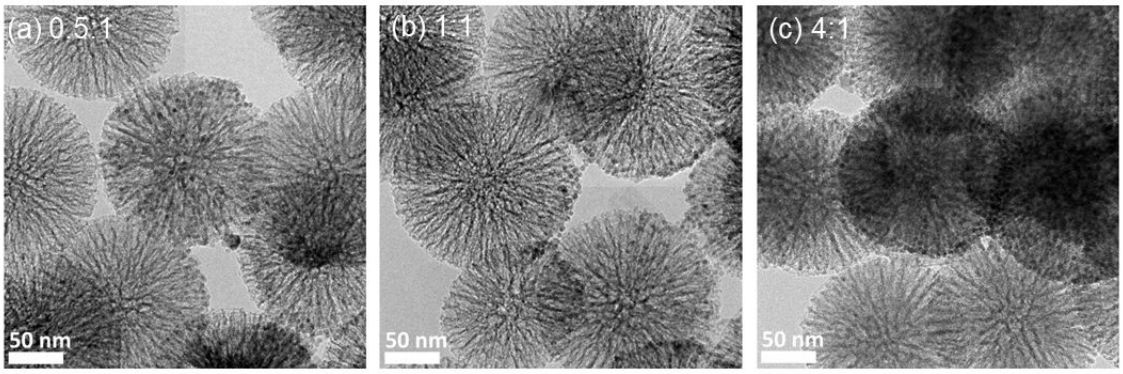

Figure S6 TEM images (a-c) of $mSiO_2$@PbS/CdS-Fe_3O_4 with various mass ratio of PbS/CdS QDs and Fe_3O_4 NPs (PbS/CdS: Fe_3O_4 = 0.5:1, 1:1 and 4:1).

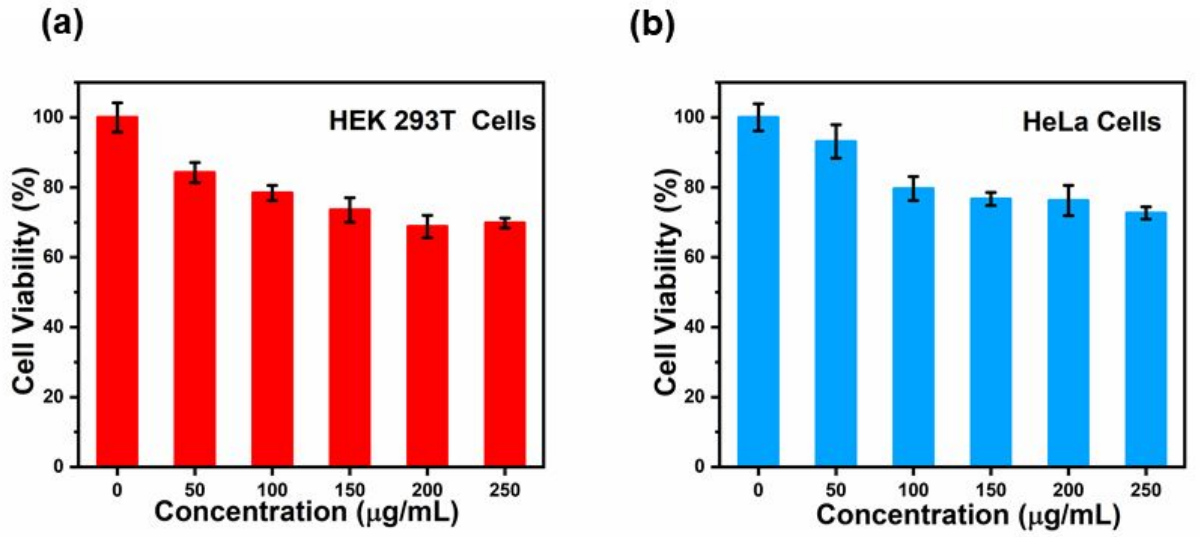

Figure S7 *In vitro* cytotoxicity study of HEK 293T (a) and HeLa (b) cells cultured with various concentrations of $mSiO_2$@PbS/CdS-Fe_3O_4 particles.

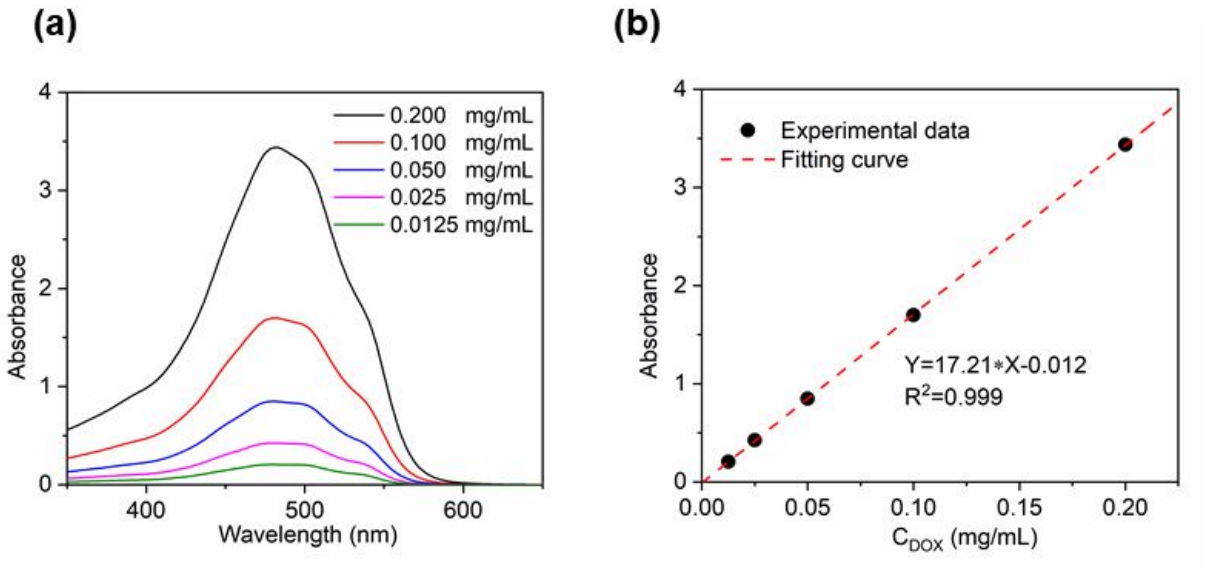

Figure S8 (a) Absorption spectra of aqueous DOX solutions at various known concentrations. (b) The linear fitting curve of absorption as a function of DOX concentration based on experimental data in (a).

Linear fitting of experimental data: $Y=17.21*X-0.012$, $R^2=0.999$.

Calculation of the concentration of DOX: $C_{DOX}= (Y+0.012)/17.21$, where Y is the absorption value at 480 nm determined by a UV-vis spectrometer.

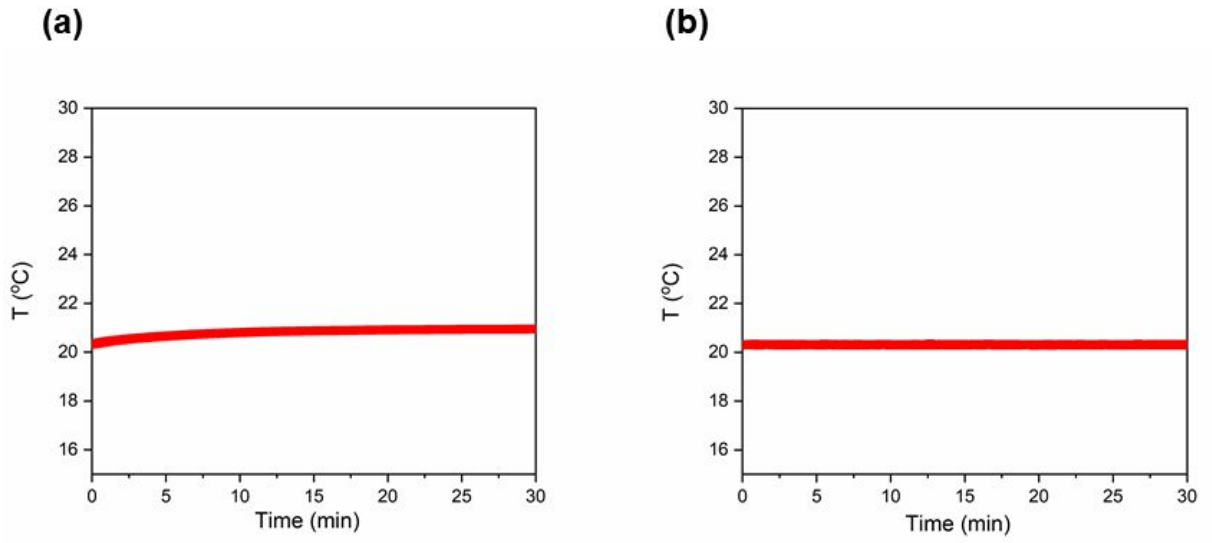

Figure S9 (a) Time-dependent temperature curves of PBS solution under two types of modulation: (a) Laser at 1.3 W/cm^2 and (b) MF at 5 kA/m.

References:

1. Park, J.; An, K.; Hwang, Y.; Park, J. G.; Noh, H. J.; Kim, J. Y.; Park, J. H.; Hwang, N. M.; Hyeon, T., Ultra-Large-Scale Syntheses of Monodisperse Nanocrystals. *Nat. Mater.* **2004,** 3, 891-5.

2. Cademartiri, L.; Bertolotti, J.; Sapienza, R.; Wiersma, D. S.; Freymann, G.; Ozin, G. A., Multigram Scale, Solventless, and Diffusion-Controlled Route to Highly Monodisperse PbS Nanocrystals. *J. Phys. Chem. B* **2006,** 110, (2), 671-673.

3. Ren, F.; Zhao, H.; Vetrone, F.; Ma, D., Microwave-Assisted Cation Exchange toward Synthesis of Near-Infrared Emitting PbS/CdS Core/Shell Quantum Dots with Significantly Improved Quantum Yields through a Uniform Growth Path. *Nanoscale* **2013,** 5, 7800-4.

4. Shen, D.; Yang, J.; Li, X.; Zhou, L.; Zhang, R.; Li, W.; Chen, L.; Wang, R.; Zhang, F.; Zhao, D., Biphase Stratification Approach to Three-Dimensional Dendritic Biodegradable Mesoporous Silica Nanospheres. *Nano Lett.* **2014,** 14, 923-932.

5. Lu, Z.; Gao, C.; Zhang, Q.; Chi, M.; Howe, J. Y.; Yin, Y., Direct Assembly of Hydrophobic Nanoparticles to Multifunctional Structures. *Nano Lett.* **2011,** 11, 3404-3412.